



# Studies on heat treatment and electrochemical behaviour of 3D printed DMLS processed nickel-based superalloy

B. Anush Raj<sup>1</sup> · J. T. Winowlin Jappes<sup>1</sup> · M. Adam Khan<sup>1</sup> · V. Dillibabu<sup>2</sup> · N. C. Brintha<sup>3</sup>

Received: 23 July 2019 / Accepted: 17 September 2019 / Published online: 23 September 2019  
© Springer-Verlag GmbH Germany, part of Springer Nature 2019

## Abstract

Additive manufacturing and its process involved during manufacturing of engineering components are thriving areas in current researches. The usage of Direct Metal Laser Sintering (DMLS) process, can resolve the difficulties involved in the manufacturing of components used with turbine engines. The commercially available alloy Inconel 718 is compatible with DMLS based Inconel 718 material. This investigation examines and experiments the effect of heat treatment process, using a combination of solutionizing at 1100 °C (2h) and aging at 845 °C for 24h, followed by air cooling. The metallurgical changes were observed with the help of optical imaging, to perceive the phase/structural transformation. Further, the heat treated samples were subjected to electrochemical polarization studies with 1.0 M H<sub>2</sub>SO<sub>4</sub> as an electrolyte. The influence of alloying elements, before and after the heat treatment process of samples were analysed through scanning electron microscope and energy dispersive spectroscopy. The experimental results prove that, corrosion resistance was found to be much better while following the sequence of DMLS HT > Bare DMLS > Bare Commercial > Commercial HT alloy. However, the heat treated DMLS sample obtained during experimentation had lower current density and more positive corrosion potential than the commercial alloys.

## 1 Introduction

Nowadays, additive manufacturing (AM) processes play a vital role in producing difficult to manufacture engineering components at an easier rate. The additive manufacturing process offers several merits towards mechanical and metallurgical properties when compared to traditional manufacturing processes. Some of the highlights of AM processes are, material efficiency, resource efficiency and production flexibility. Satish et al, in their work reported that, designing a product using Additive Manufacturing process leads to optimal and accurate results when compared to usage other conventional machining process [1]. Mohsen et al. claimed

that, the mechanical properties of AM are controlled by feed stock powder and process parameters such as scan direction, part placement, inert gas flow velocity, scan strategy and build direction, laser power scan speed, scan spacing and bed temperature. By increasing the laser intensity (density), the porosity of specimen can be reduced [2]. The process of additive manufacturing constructs bulk material, as layer by layer of fused metal to produce complex geometric shapes with fully dense material. In general, additively manufactured metals have good mechanical properties [3]. The nickel-based superalloys are found to have wide applications in aerospace, gas turbine engine, nuclear reactors, boilers and medical unit manufacturing. Additive manufacturing process creates complex shapes using 3D geometric data, directly through CAD models of the components. This process is an automated manufacturing process which is similar to rapid prototyping [1].

IN718 nickel alloy has enough amount of chromium, niobium, molybdenum, aluminium and titanium to meet the requirements. The addition of heavy metals such as Co, Mo and W, improves the mechanical strength of superalloy [4]. The increase in niobium content improves the corrosion resistance of super alloys. The combination of niobium with oxygen, leads in the formation of niobium oxide layer

✉ M. Adam Khan  
adamkhanm@gmail.com

<sup>1</sup> Department of Mechanical Engineering and Centre for Surface Engineering, Kalasalingam Academy of Research and Education, Virudhunagar, Tamilnadu, India

<sup>2</sup> Small Turbo Fan Section, Gas Turbine Research Establishment (GTRE), DRDO, Bangalore, India

<sup>3</sup> Department of Computer Science and Engineering and Centre for Surface Engineering, Kalasalingam Academy of Research and Education, Virudhunagar, Tamilnadu, India

which protects and increases the passive current density of the material [5]. The IN718 superalloys are recommended for their ability to withstand aggressive corrosive environment while operating at different temperatures. Due to the above advantages, these alloys are widely used in manufacturing of gas turbine blades [1]. The additively manufactured components require appropriate heat treatment process, to enhance the quality in terms of mechanical properties and resistance towards corrosion [6]. Annealing or solution treatment process is required for additively manufactured component, to refine grain and achieve improved creep resistance [7]. These combination of alloys in the form of annealing and age-hardening form  $\gamma'$  phase with the precipitation as  $\text{Ni}_3(\text{Al},\text{Ti})$  phase and  $\gamma''$  phase as  $\text{Ni}_3\text{Nb}$  phase would enhance the desired properties of the material.

The research gaps identified from the other reviewed literatures are, the simulation of electrochemical behaviour of superalloy with  $\text{H}_2\text{SO}_4$  solution have not been exposed in many aspects. At the same time, the development of samples through AM process and electrochemical behaviour were not reported in any literature.

Thus, the electrochemical corrosion resistance of IN718 superalloy obtained through the use of direct metal laser sintering (DMLS) and conventional casting were studied and experimented in this work. To analyse the metallurgical property, the sample were examined with and without heat treatments. In addition, the results obtained after experimentation were compared through optical metallography, electron microscopy and energy-dispersive X-ray spectroscopy.

## 2 Experimental

The studies on electrochemical behaviour were carried out using nickel-based superalloy, produced through direct metal laser sintering (DMLS) and commercially available alloy. The composition of commercially available IN718 alloy is shown in (Table 1).

The DMLS samples were fabricated using EOS M280 DMLS machine. The optimum process parameters used are: power of 285 W; scan rate of 970 mm/s; hatching distance 0.15 mm; layer thickness 40  $\mu\text{m}$ ; and beam diameter of 0.08 mm.

### 2.1 Heat treatment

The DMLS samples were heat treated to refine grain structure. Heat treatments were performed using tubular furnace.

The test samples were heat treated with a combination of two temperatures and heat treatment process which includes annealing and age hardening. The heat treatment process was carried out on the samples by solutionizing at 1100  $^\circ\text{C}$  for 2 h and then by age hardening with temperature at 845  $^\circ\text{C}$  for 12h [8, 9]. This procedure is being followed for commercially available superalloys. The changes in metallurgical structure after heat treatment were studied using microstructure analysis. To test this process, the specimens were prepared and etching was carried by 87 Glyceregia (ASTME 407 STD).

For performing potentiodynamic polarization, the polished samples were cleaned with ethanol before exposure. The electro chemical behaviour of the above samples were analysed using 1.0M  $\text{H}_2\text{SO}_4$  solutions [10]. ASTM G3-14 standard was followed with corrosion cell exposed area of 1  $\text{cm}^2$ . Calomel and platinum are the two electrodes which can be used with the potential of  $-250$  mV to 250 mV at 1 mV/s as sweep rate to measure potential–current density. Then the exposed surface was subjected to metallurgical analysis using electron microscope and X-ray spectroscopy. Various experimental analysis were done to analyze the performance of material.

## 3 Results and discussions

### 3.1 Metallographic study

The bare DMLS sample possess more build tracks throughout the surface. Molten pools are found in multi-tracks and these tracks overlap in horizontal direction called track—track boundaries. The optical image of DMLS bare metal, before heat treatment is shown in Fig. 1a. The formation of bi-directional dendrite structure during the solidification process, was a major observation found in bare sample. Temperature gradient and sintering condition decides the texture solidification of the bare component. The surface morphology of the heat treated DMLS processed IN718 were observed in optical metallography (OM). Thus, this phase makes the material to have anisotropic condition with respect to the built tracks. To improve the anisotropic behaviour of the samples, they were subjected to heat treatment. The optical image of the commercially available alloy, before heat treatment process is depicted in Fig. 1b. In commercial alloy, after heat treatment metallurgical changes were found in higher order. Figure 2a shows the microstructure and metallurgical changes in DMLS sample after heat

**Table 1** Composition of IN718 superalloy

Element	Ni	Fe	Cr	Nb	Mo	Ti	Al	Si	C	Co	Cu	W
Weight %	52.44	19.78	17.13	4.77	3.38	1.11	0.59	0.13	0.05	0.16	0.23	0.23

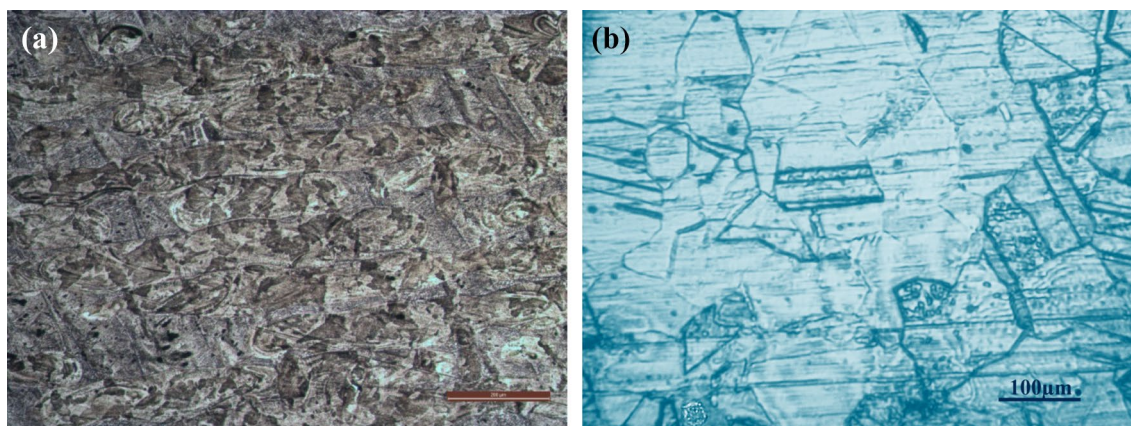


**Fig. 1** Optical image of bare material; **a** DMLS alloy; **b** commercial alloy

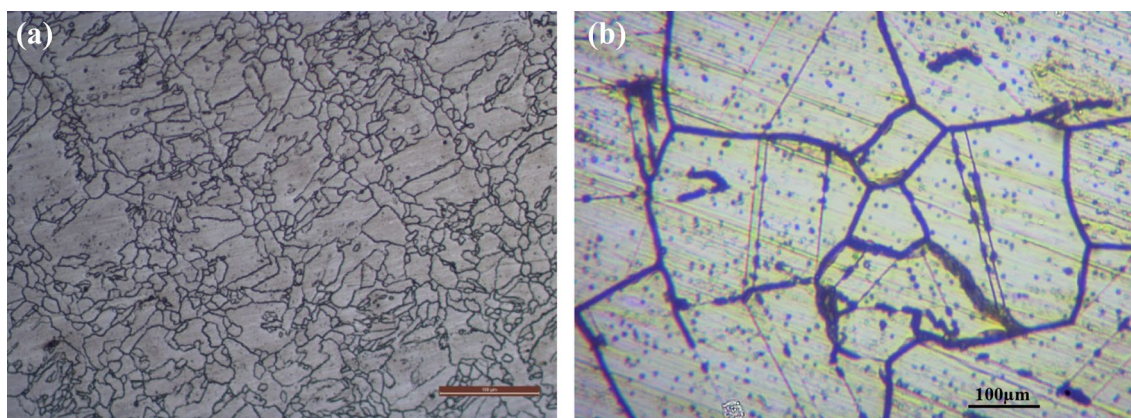


**Fig. 2** Optical image of heat treatment materials. **a** DMLS alloy; **b** commercial alloy

treatment plan (combination of solutionising at 1100 °C for 2 h and age hardening at 845 °C for 12 h). A large number of columnar grains were formed in the DMLS sample, which leads to isotropic property. After heat treatment process, fine grains were formed at the build track of melt zone followed by nodular/columnar grains in between the hatch space. The optical image of heat-treated commercial alloy is shown in Fig. 2b. The structure reveals the twinning effect on heat treatment with respect to the commercial alloy. The changes observed in the structure is due to the effect of heat and induced grains which glides with each other. Due to this treatment, the mechanical strength of the alloy may increase, but it is sensitive to metallurgical behaviour on aggressive environment.

It has to be highlighted that, during the heat treatment process the metallurgical structure of both the alloys had wide transformations. The grain refinements and phase transformations identified were the major results. The comparison of XRD diffractogram of commercial and DMLS (before and after heat treatment) is shown in Figure 3. The

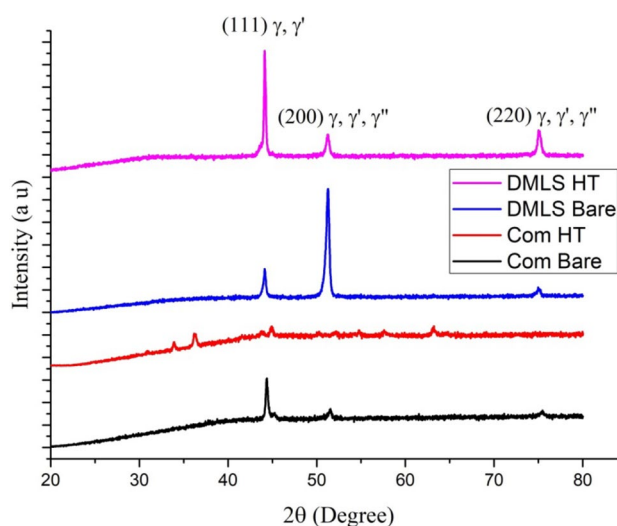


**Fig. 3** Comparison of XRD diffractogram of heat treated commercial and DMLS IN718 alloy

formation of  $\gamma$ ,  $\gamma'$  and  $\gamma''$  precipitations were found to be better in DMLS processed alloy when compared to commercially available alloy [11]. In addition, the inherent properties of DMLS alloy was found to be increased. The evidence for precipitation of  $\gamma$ ,  $\gamma'$  and  $\gamma''$  phase peaks, were obtained at an angle  $44.1^\circ$ ,  $51.2^\circ$  and  $75.05^\circ$ ; with an intensity of 1144 a.u. (bare commercial alloy); 293 a.u. (heat treated commercial alloy); 800 a.u (bare DMLS alloy) and 2819 a.u. (heat treated DMLS alloy) respectively. The intensity was found to be very low for commercial alloy when compared to DMLS alloy which provides an indication on the improvement of metallurgical quality and mechanical strength as a result of phase transformation.

### 3.2 Electrochemical polarization

The influence of heat-treated samples were investigated with electrochemical polarisation analyser for examining the corrosion behaviour of the samples. The kinetics of cathodic and anodic reaction of alloy at 1.0M  $H_2SO_4$  solution was inferred. The volt-ampere graphs were obtained from potentiodynamic polarization. Performance comparison were carried out to analyse the effect of heat treatment on DMLS samples and commercial alloys. From the graph depicted in (Figure 4) potential ( $E_{corr}$ ) and current density ( $I_{corr}$ ) were identified and tabulated in Table 2.

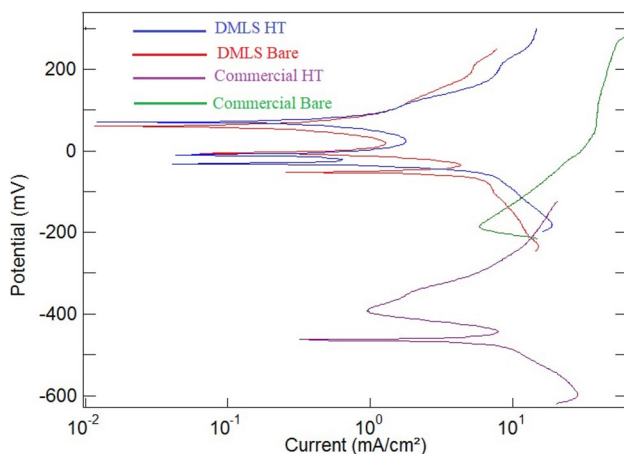


**Fig. 4** Potentiodynamic polarization graph obtained from inbuilt software

**Table 2** Potentiodynamic polarization data

Material	Rest potential $R_p$ (mV)	Corrosion potential $E_{corr}$ (mV)	Current density $I_{corr}$ (mA/cm <sup>2</sup> )	Corrosion rate $C_R$ (mm/year)
Commercial bare	3.19	- 202.46	1.3142	23.116
Commercial HT	- 369.91	- 403.11	1.3868	24.393
DMLS bare	- 0.73	- 9.9925	0.8074054	14.202
DMLS HT	42.16	- 9.7224	0.6188507	10.885

The corrosion density ( $I_{corr}$ ) was found to be maximum for commercial heat treated alloy ( $1.386 \text{ mA/cm}^2$ ) followed by commercial plain ( $1.3142 \text{ mA/cm}^2$ ), plain DMLS ( $0.807405 \text{ mA/cm}^2$ ) and DMLS heat treated samples ( $0.61885 \text{ mA/cm}^2$ ). Commercial alloy was found to have high current density while compared to DMLS alloy. This process reveals the insignificant variation between heat treated and plain samples.

The commercial alloy, bare and heat-treated samples possess less cathodic reaction and has produced high corrosion rate. The DMLS alloy, both bare and heat-treated sample have high cathodic reaction with less corrosion rate. The corrosion rate of DMLS alloy has almost reduced to 50% when compared to commercial alloys. These significant metallurgical changes were found to be the predominant factors for improvement in corrosion resistance of the treated material.

The cathodic current from the potentiodynamic polarization curve was higher in case of commercial alloy. The current density and corrosion potential were found to be maximum for DMLS alloy when compared to commercial alloy. The heat treated DMLS alloy, provides better corrosion resistance and corrosion rate when compared commercial alloy.

### 3.3 Surface properties

The surface morphology of the sample exposed to 1.0 M  $H_2SO_4$  solution using electrochemical corrosion analysis is shown in Fig. 5. The behaviour of the materials were invariant with reference to heat treatment process. Figure 5 shows the effect of corrosive medium on the exposed surface of alloys. In commercial alloy (bare metal), the surface degradation was found aggressive with severe metal loss. Dimples that were found over the commercial alloy, revealed to be larger in size. The electrochemical reaction of the corrosive medium on heat treated sample (of commercial alloy) was found allied over grain boundaries. This was due to thermal stress induced on the surface of the material [12]. On analysing the heat treated samples, the grain boundaries were highly prone to severity in corrosion which was clearly identified through SEM micrograph. However, the common autocatalytic reaction was noticed in the DMLS alloys (for both bare and heat-treated samples) in the form of pitting.

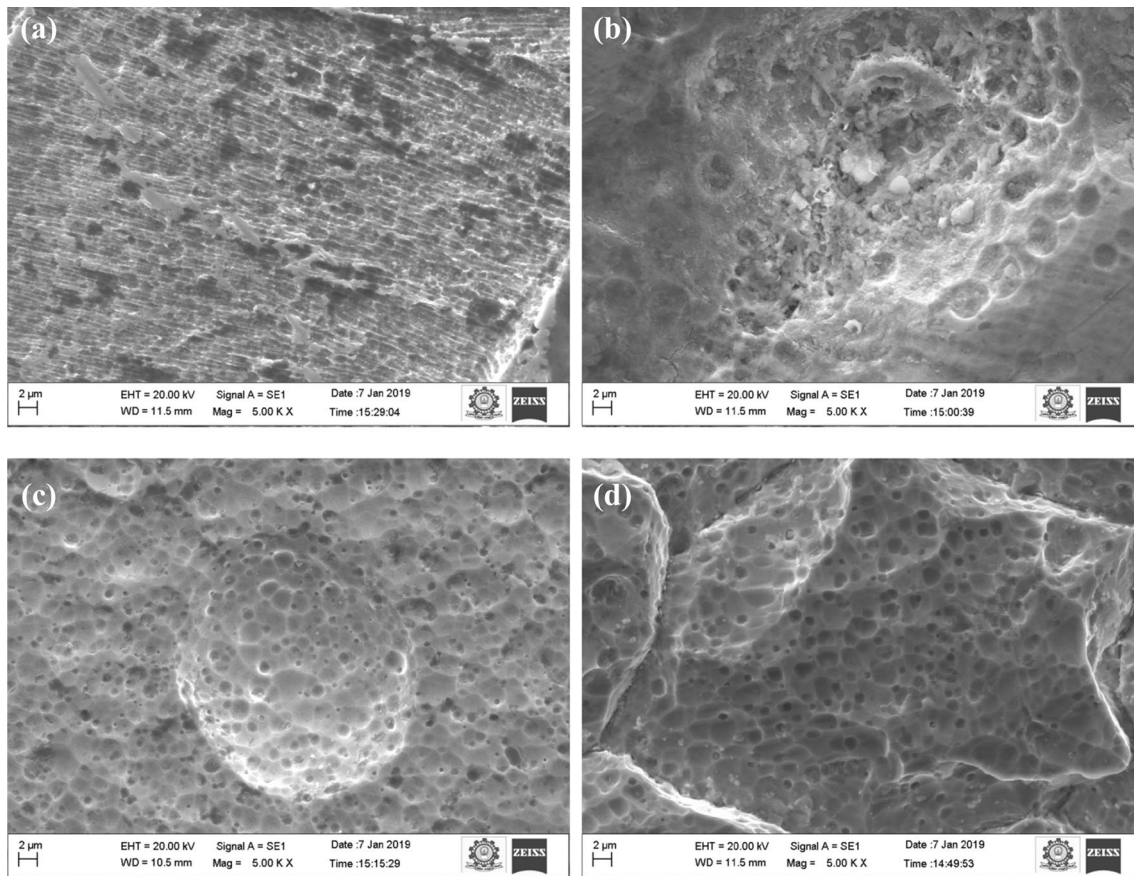


**Fig. 5** SEM image corrosion morphology: **a** DMLS Bare; **b** DMLS heat treated; **c** commercial bare; **d** commercial heat treated

The rate of pitting was highly significant with reference to the metallurgical quality of the alloy. However, in DMLS sample uniform corrosion was revealed as shown in Fig. 5a.

Further, the effect and influence of alloying elements in the material were discussed with EDS results. On exposure to the corrosive medium, the segregation of the alloying elements such as molybdenum, titanium and niobium of DMLS heat treated alloy was found to be very high when compared to commercial heat treated alloys. From the EDS analysis it is evident that, Nb, Mo, Ti and Al element precipitation was found to be high and in DMLS sample, the  $\gamma'$  and  $\gamma''$  precipitation has been increased. Figure 6 infers the spectrum and mapping of DMLS heat treated samples. The major element on the exposed area is Fe and Cr along with Ni. This is because of the kinetic reaction of sulphur with the metallic element. Contribution of Mo and Nb are equally reacting with corrosion medium in order to protect the surface from corrosion. The corrosion resistance was found to increase due to the segregation of these elements. Figure 7 exhibits the element segregation of commercial heat treated samples. When compared to commercial heat treated alloy, the iron precipitation was found to be higher than the heat treated DMLS alloy which leads to dissolution of anodic rate. The

corrosion current decreases with decrease of iron element [13]. The iron precipitation was found to be high of about 54% in commercial heat treated alloy whereas in DMLS heat treated alloy the iron precipitation was about 17%. The precipitation of iron was found to be high in commercial heat treated alloy whereas the nickel precipitation was high in DMLS heat treated alloy. As a summary, the performance of DMLS route base material was found to outperform better than the commercially available superalloys. On further heat treatment, the metallurgical quality of the material was found to have significant changes with reference to time, temperature and its transformation.

## 4 Conclusions

The above investigations were made as per the plan, to study and analyse the metallurgical changes and electrochemical behaviour of DMLS superalloy and commercially available IN718. The outcomes of experimentation are as follows:

- The DMLS samples are anisotropy in nature, in bare condition. Variation in bulk property was based on the build

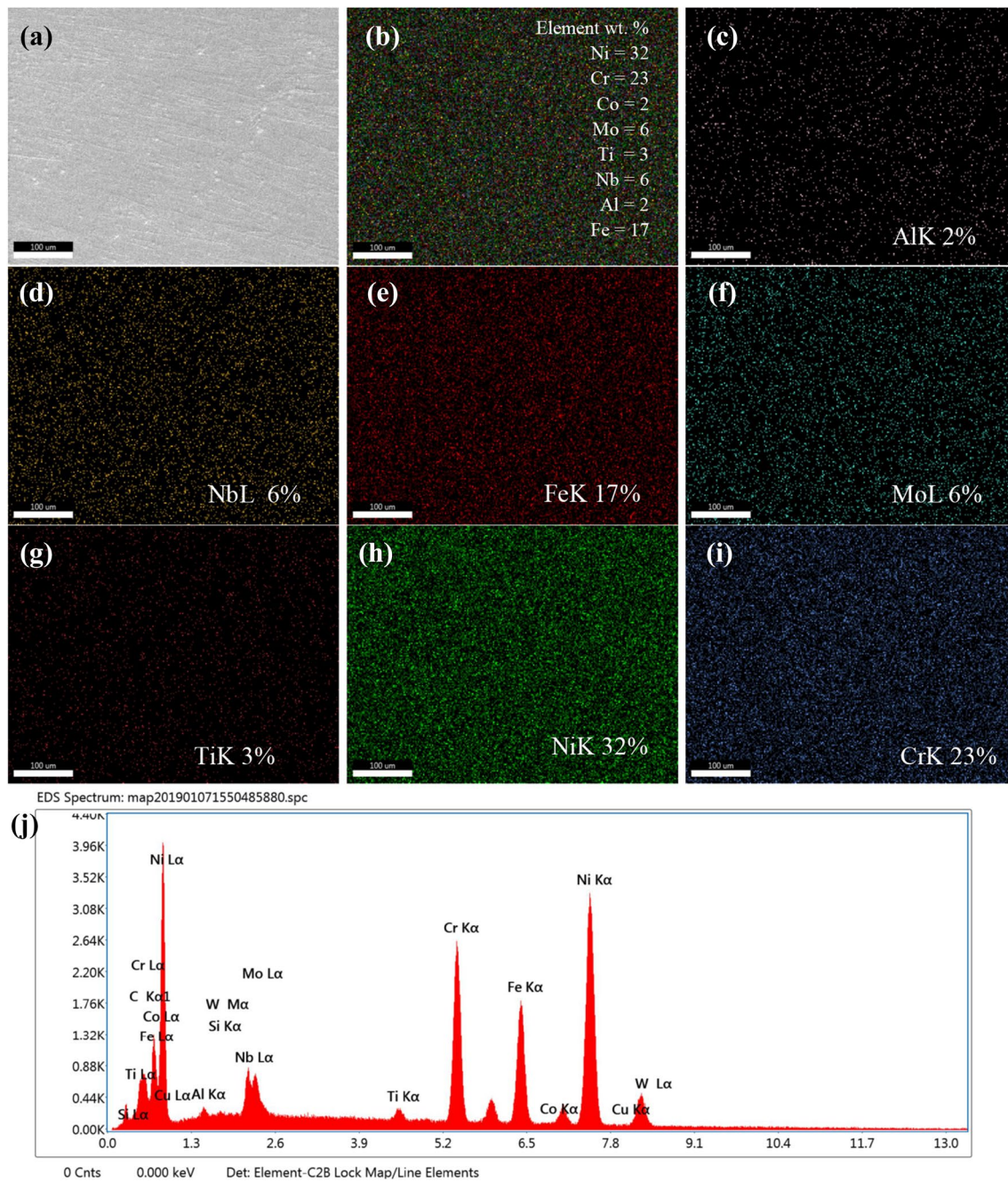


**Fig. 6** EDS Mapping of exposed DMLS heat treated sample; **a** SEM image; **b** element composition; **c** distribution of aluminium; **d** distribution of niobium; **e** distribution of iron; **f** distribution of molybde-

num; **g** distribution of titanium; **h** distribution of nickel; **i** distribution of chromium; **j** element spectra

direction and the number of layers. On heat treatment, DMLS sample has changed to isotropy nature with uniform grain structure.

- The homogenization of DMLS material has produced austenitic phase (FCC structure) which is common in commercially available alloy.
- With reference to electrochemical corrosion, there is no significant difference on corrosion rate in commercial

alloy. However, the corrosion rate in DMLS samples was found to be better than the commercial alloy.

- Based on the corrosion potential, heat treated commercial alloy was found to possess high susceptibility towards corrosion, whereas DMLS alloy has medium and minimum susceptibility towards corrosion. As an output, grain boundary of the heat treated commercial

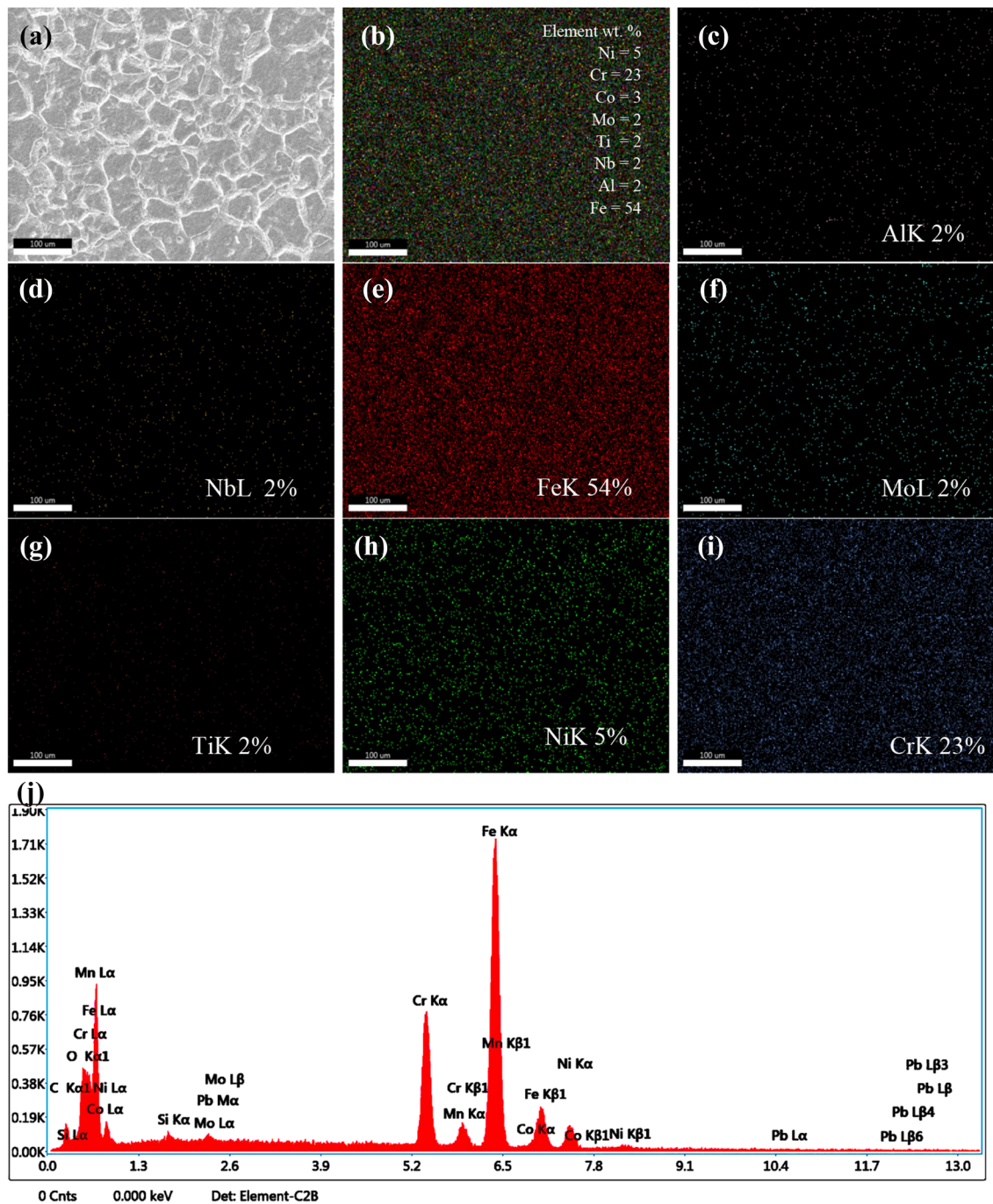


**Fig. 7** EDS mapping of corroded commercial heat treated sample. **a** SEM image; **b** element composition; **c** distribution of aluminium; **d** distribution of niobium; **e** distribution of iron; **f** distribution of molyb-

denum; **g** distribution of titanium; **h** distribution of nickel; **i** distribution of chromium; **j** element spectra

alloy has been induced with intergranular corrosion in combination with pitting.

Therefore, the heat treated DMLS sample, has high potential to protect the material from aggressive corrosion and material loss on exposure to 1.0M H<sub>2</sub>SO<sub>4</sub>.

## References

1. K. Satish Prakash, T. Nancharaih, V. V. Subba Rao, Additive manufacturing techniques in manufacturing—an overview. *Mater. Today Proc.* **5**, 3873–3882 (2018)

2. Mohsen Mohammadi, W. Rubio, M. Mousseigne, T. Sultan, F. Rezai, Achieving low surface roughness AISi10Mg 200C parts using direct metal laser sintering. *Addit. Manuf.* **20**, 23–32 (2018)
3. E. Chlebus, K. Gruber, B. Kuźnicka, J. Kurzac, T. Kurzynowski, Effect of heat treatment on microstructure and mechanical properties of Inconel 718 processed by selective laser melting. *Mater. Sci. Eng. A*. <https://doi.org/10.1016/j.msea.2015.05.035>
4. Mohamed Retima, Saida Bouyegh, Hacène Chadli, Effect of the heat treatment on the microstructural evolution of the nickel based Superalloy. *Metalurgija-MJoM* **17**(2), 71–77 (2011)
5. N. D. Nam, J. G. Kim, Effect of niobium on the corrosion behaviour of low alloy steel in sulfuric acid solution. *Corros. Sci.* **52**, 3377–3384 (2010)
6. C.A. Huang, T.H. Wang, W.C. Han, C.H. Lee, A study of the galvanic corrosion behavior of Inconel 718 after electron beam welding. *Mater Chem Phys* **104**(2–3), 293–300 (2007)
7. G. Marchese, E. Bassini, M. Calandri, E. P. Ambrosio, F. Calignano, M. Lorusso, D. Manfredi, M. Pavese, S. Biamino, P. Fino, Microstructural investigation of as-fabricated and heat treated Inconel 625 and Inconel 718 fabricated by direct metal laser sintering, *Metal Powder Rep.*
8. N. El-Bagoury, Microstructure and mechanical properties of aged nickel base superalloy. *Arch. Appl. Sci. Res.* **3**(2), 266–276 (2011)
9. N. El-Bagoury, M.A. Amin, Q. Mohsen, Effect of various heat treatment conditions on microstructure, mechanical properties and corrosion behavior of Ni base superalloys. *Int. J. Electrochem. Sci* **6**, 6718–6732 (2011)
10. M.A. Khan, Electrochemical polarisation studies on plasma-sprayed nickel-based superalloy. *Appl Phys A* **120**(2), 801–808 (2015)
11. X. Li, J.J. Shi, C.H. Wang, G.H. Cao, A.M. Russell, Z.J. Zhou, G.F. Chen, Effect of heat treatment on microstructure evolution of Inconel 718 alloy fabricated by selective laser melting. *J Alloy Compd* **764**, 639–649 (2018). <https://doi.org/10.1016/j.jallcom.2018.06.112>
12. X. Li, F. Xie, D. Wang, C. Xu, M. Wu, D. Sun, J. Qi, Effect of residual and external stress on corrosion behaviour of X80 pipeline steel in sulphate-reducing bacteria environment. *Eng Fail Anal* **91**, 275–290 (2018). <https://doi.org/10.1016/j.engfailana.1.2018.04.016>
13. R.R. Sayano, K. Nobe, Electrochemical and corrosion behavior of Fe–Ni alloys in sulfuric acid. *Corrosion* **25**(6), 260–266 (1969)

**Publisher's Note** Springer Nature remains neutral with regard to jurisdictional claims in published maps and institutional affiliations.